FRACTURE TOUGHNESS ENHANCEMENT WITH REINFORCING FIBERS FOR ADHESIVELY BONDED JOINTS UNDER REPEATED THERMAL SHOCKS

C.S.Bang[1], J.G. Kim[1], D.G. Lee[1]*
[1]School of Mechanical Aerospace & Systems Engineering, Korea Advanced Institute of Science and Technology, ME3221, Guseong-dong, Yuseong-gu, Daejeon 305-701, Republic of Korea,

* Corresponding author (dglee@kaist.ac.kr)

Keywords: *Fiber reinforcement; fracture toughness; metal foil joint; repeated thermal shock.*

1. Introduction

Cryogenic containment systems for liquefied natural gas (LNG) ships are generally composed of primary and secondary barriers [1]. The primary barrier consists of welded metallic plates, while the secondary barrier is constructed by adhesively bonded thin metal foils to reduce thermal stresses during cool down period as shown in Fig.1.

In this work, the bonding performance of adhesively bonded secondary barrier, which seals the gap between the insulation panels composed of aluminum face with foam core and stainless foils, was investigated with respect to the adhesive thickness. The adhesive thickness control in the adhesively bonded joint for the secondary barrier is not easy in real applications due to level differences between insulating panels. To improve the bonding performance under repeated thermal shock, the adhesive of joints was reinforced with glass fibers. The bonding strengths of single lap joints using fiber-reinforced film adhesive were measured with respect to the adhesive thickness and fiber volume fraction at the cryogenic temperature. Also, the Mode I fracture toughness of adhesively bonded joints was measured using double cantilever beam (DCB) specimen.

From the experimental results, a suitable adhesive thickness of adhesively bonded metal joints as well as optimum volume fraction of fiber were suggested for the robust adhesive joint against repeated thermal shock.

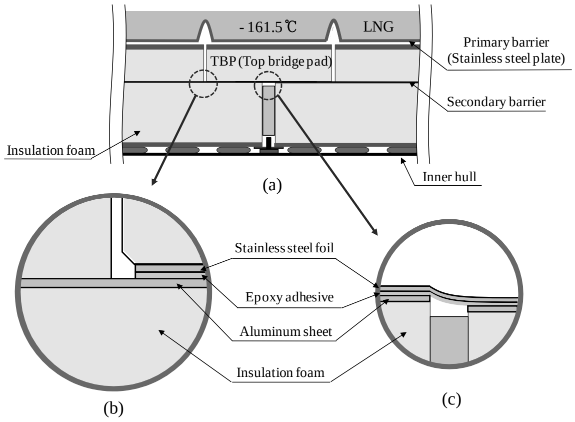

Fig. 1. Schematic diagrams of LNG containment system composed of the primary and secondary barriers: (a) overall drawing; (b) enlarged view at the corner of top bridge pad; (c) insulation panels with level difference.

2. Experiment

2.1. Material properties

Fully annealed aluminum plates (1050-O) and stainless steel plates (SUS 304L) were prepared for the adherends of single lap shear test and double cantilever test, whose material properties were listed in Table 1. The metal foils were bonded using a film adhesive (FM8210-1M, Cytec, U.S.A.) with different adhesive thicknesses of 0.05 ~ 1.0 mm. Table 2 lists the cured adhesive properties. The curing temperature and time were 90℃ and 4 hours, respectively under the curing pressure of 0.1 MPa.

Table 1 Material properties of the fully annealed aluminum foil and stainless steel foil

Materials	Aluminum foil (1050-O)	Stainless steel foil (304L)
Modulus (GPa)	70	198
Yield strength (MPa)	32	269
Tensile strength (MPa)	84	731
Failure strain (%)	43	42

Table 2 Material properties of the film adhesive

Materials	Film adhesive
Modulus (GPa)	4.2
Tensile strength (MPa)	96.6
Failure strain (%)	3.5
Poisson's ratio	0.43
Density (kg/m^3)	1120

2.2. Surface treatment

The aluminum and stainless steel foils were flame treated and then immersed in the γ-glycidoxypropyl-trimethoxysilane (GPS) solution, to improve the adhesion strength at the cryogenic environment [2,7]. The flame treatment using propane (C_3H_8) gas was conducted to eliminate surface contaminants such as adsorbed machine oil and other lubricants on the metal surfaces during manufacturing. The surface temperature of flame with this equipment was about 900℃. The treatment time was 5 seconds.

2.3 Test method modification

2.3.1 Lap shear test

The bonding strength of single lap joints was measured with respect to the adhesive thickness from 0.05 to 1.0 mm based on the ASTM D1002 [3]. In order to simulate the actual thermo-mechanical behavior of the insulation panel, the aluminum and stainless foil were bonded to a thick stainless block as shown in Fig. 2. The aluminum and stainless sheet were bent at the edge to avoid de-lamination failure between the metal foils and the adherend. The insulation panel is a type of sandwich construction, composed of a thin aluminum sheet secondary barrier as the face structure and a thick glass fiber reinforced polyurethane foam (RPUF) insulation as the core. The thickness of the stainless block was determined to be 20 mm considering the actual flexural rigidity of the insulation sandwich construction with dissimilar face materials [4].

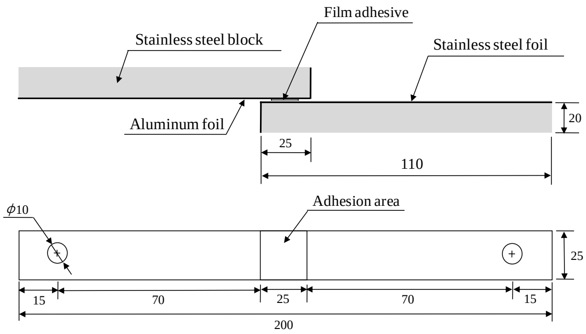

Fig. 2. Schematic drawing of the adhesively bonded metal joint specimen for single-lap shear test (dimensions in mm).

2.3.2 Double cantilever beam (DCB) test

The bonding strength of fracture toughness of Mode I was measured based on the ASTM D3433 standard as shown in Fig. 3 (a) [5]. The level spacer such as razor blade coated with the mold release were placed at the both ends of the laminate of the film-type adhesive to control adhesive thickness as shown in Fig. 3(b). Then the DCB specimens were cured at 90^{o}C for 4 hours under 0.1 MPa pressure in a hot-press. The spacer was removed and then the sharp initial crack tip in the adhesive layer was generated by tapping the fresh razor blade [6].

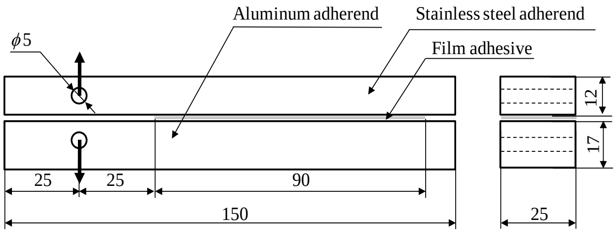

(a)

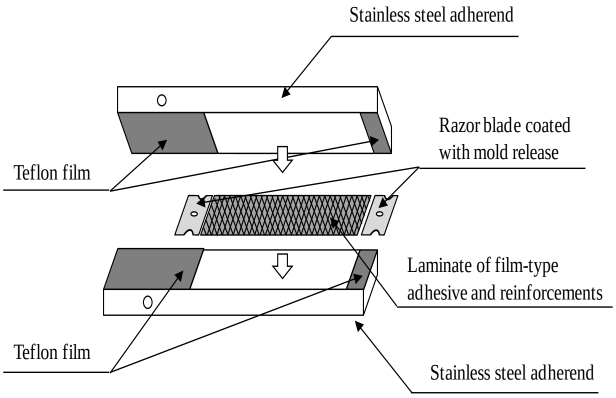

(b)

Fig. 3. Schematic drawing of the adhesively bonded metal joint specimen for DCB test (dimensions in mm): (a) test specimen; (b) fabrication process.

Because the substrates had different flexural rigidities from material differences, the DCB specimen did not deform symmetrically and the tensile forces are no longer normal to the crack surface [9]. In this study, the modified test method was applied with dissimilar substrates of different thickness [10]. The deflection of a cantilever beam is given by

$$\delta = \frac{Pa^3}{3EI} \quad (1)$$

where *EI* is the flexural rigidity, *a* and *P* are the length and concentrated load, respectively. To have the same deflection for each substrate, the flexural rigidity should be the same as follows;

$$(EI)_{\text{stainless steel}} = (EI)_{\text{aluminum}} \quad (2)$$

In this study, the thicknesses of 12 mm and 17 mm were chosen for the aluminum and the stainless, respectively.

3. Test results

3.1 Effect of adhesive thickness

Fig. 4 represents the measured lap shear strength at -150℃ with respect to the thickness of adhesive, where the bond strengths decreased almost linearly as the adhesive thickness was increased. When the adhesive thickness of the single lap joint was 1.0 mm, the lap shear strength decreased 50.4 % compared to that of single lap joint with the adhesive thickness of 0.15 mm. This phenomenon could be explained by the confinement of plastic zone by the adherends. For the thick adhesive, since the plastic zone around the crack tip was not confined much by the adherends, it had relatively low fracture toughness, whilst the plastic zone of thin adhesive was confined greatly in the adhesive layer due to proximity of the adherends [8, 9]. Additionally, the thicker adhesive might produce thermal residual stresses due to the C.T.E. (Coefficient of thermal expansion) difference between the metal and adhesive, which could reduce the joint strength, particularly at the low temperature of -150℃.

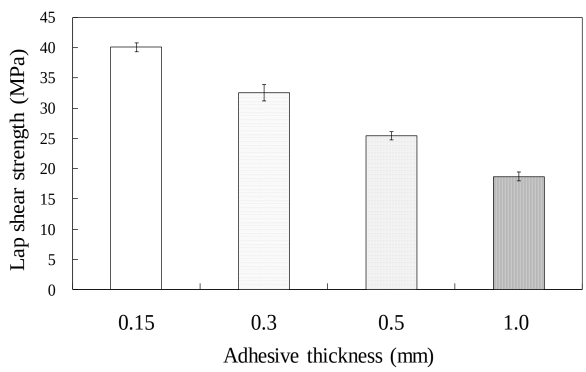

Fig. 4. Lap shear strengths of the single-lap joints at -150℃ with respect to the adhesive thickness of the adhesively bonded joints.

To investigate the ageing effect under repeated thermal shocks, thermal cycling tests in liquid nitrogen were carried out. The test specimens were immersed in the liquid nitrogen of -196℃ for 5 minutes and dried at 30℃ for 15 minutes in a temperature controlled chamber as shown in Fig. 5. In this study, thermal shock tests were conducted after 1, 100 and 300 thermal cycles considering the ship life time of 20 years. Fig. 6 shows the lap shear strengths at -150℃ after repeated thermal shocks with respect to the adhesive thickness of the adhesively bonded joints.

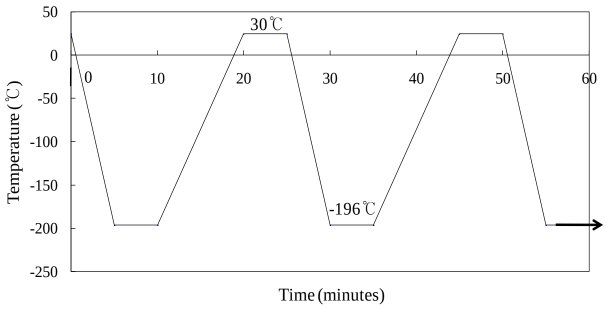

Fig. 5. Thermal cycle profile for ageing effect on the adhesively bonded joint strength.

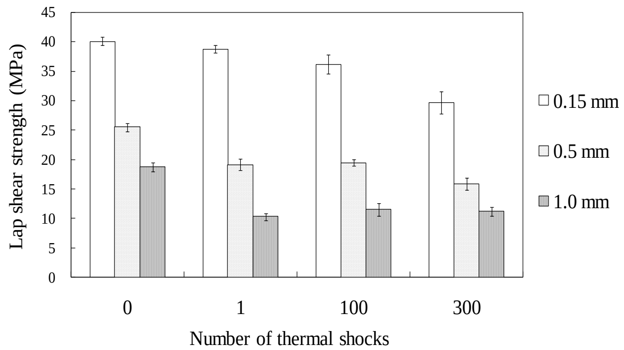

Fig. 6. Lap shear strengths of the single-lap joints at -150℃ with respect to the adhesive thickness of the adhesively bonded joints after different thermal shocks.

Three different adhesive thicknesses of the lap shear joint were selected to investigate the effect of thermal cycling. When the adhesive thickness was 0.15 mm, the lap shear strength gradually decreased by 26 % after 300 thermal shocks. However, when the adhesive thickness was 0.5 mm or 1.0 mm, the lap shear strengths decreased rapidly even after 1 thermal shock. The bond strength decreased by 27 % and 47 % after 1 thermal shock when the adhesive thicknesses were 0.5 mm and 1.0 mm, respectively. The thick adhesive might easily crack under even only 1 thermal shock due to the low fracture toughness of the adhesive layer as described previously. Consequently, the joint with large adhesive thickness had lower bond strength. On the other hand, the lap shear strength with 0.15 mm adhesive thickness decreased by 3.5 % after 1 thermal shock and gradually decreased with repeated thermal shocks. Therefore, the control of the adhesive thickness in real application would be very important for robust joint design of secondary barrier against repeated thermal shocks during the LNG ship lifetime.

3.2 Effect of fiber reinforcement

Although the adhesive thickness less than 0.2mm was recommended for robust joint design, it is not easy to control adhesive thicknesses in real application due to the level differences between insulation panels. Therefore, the method for improving bonding strength and fracture toughness should be considered in real application. In this study, the reinforcements with E-glass fiber in the adhesive layer were investigated to improve the bonding performance, especially fracture toughness of adhesively bonded metal joint. The randomly oriented E-glass fibers, which were fabricated as a mat type, were used for the reinforcement of the film type epoxy adhesive. The fiber diameter was 10 μm and the density was 2.58×10^3 kg/m^3.

Four different volume fractions of 0.0 %, 5.5 %, 10.0 % and 14.6 % were considered in this study. The adhesive thickness was controlled as 0.5 mm. Fig.7 shows the lap shear strength with respect to the fiber volume fraction at the cryogenic temperature of -150℃. Without fiber reinforcement, the adhesive joint had relatively low bonding strength with highly scattered data because the adhesive flowed out during specimen curing, which resulted in the uneven adhesive thickness. On the contrary, the lap shear strength with scrim increased significantly with little deviation due to fiber reinforcement. However the lap shear strengths were not changed considerably with respect to the E-glass fiber volume fraction because the fibers reinforced in plane direction might improve slightly the lap shear strength in the transverse shear mode.

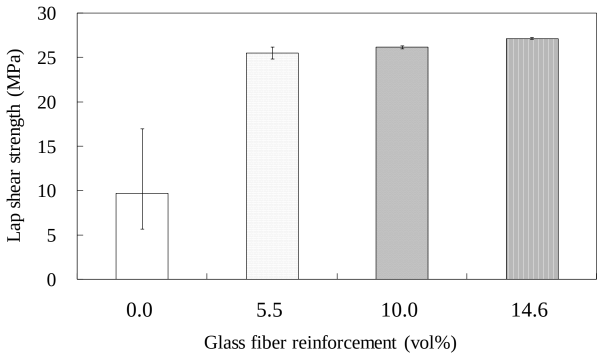

Fig. 7. Lap shear strengths of the single-lap joints at -150℃ with respect to the fiber volume fraction for 0.5 mm adhesive thickness.

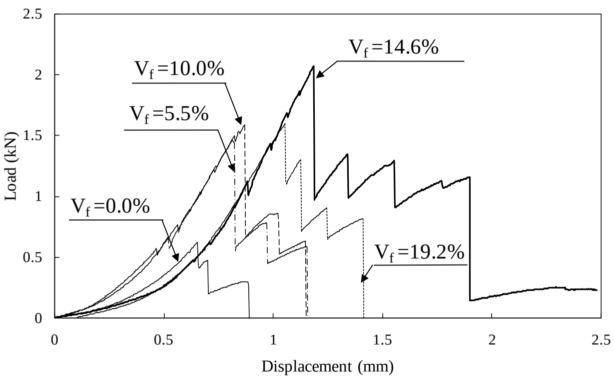

Fig. 8. Typical load-displacement curves of the DCB adhesive joint bonded with the film-type adhesive with respect to the fiber volume fraction at -150℃.

Fig. 8 shows the load-displacement curves of the DCB test with respect to the fiber volume fraction of E-glass fibers at the cryogenic temperature of -150°C. As shown in the curves, the reinforced fiber in the adhesive not only increased the fracture loads, but also retarded the crack propagations. The critical energy release rate, G_{Ic}, [J/m^2] was calculated as follows [5,11]:

$$G_{Ic} = \frac{4P^2(3a^2 + h^2)}{EB^2h^3} \tag{3}$$

where P is the load to start crack [N], E is the tensile modulus of adherend [MPa], B is the specimen width [mm], a is the distance from crack tip to pin hole centers [mm], and h is the thickness of adherend [mm]. The magnitudes of G_{Ic} of the DCB adhesive joints for 5.5 %, 10.0 %, 14.6 % and 19.2 % were 2.2, 2.4, 3.0 and 2.6 times higher than unreinforced adhesive, respectively at the initial crack start points. In this study, it was concluded that the optimum fiber volume fraction of randomly oriented E-glass fiber mat was 14.6 %.

4. Conclusion

In this study, the cryogenic joint strength of the adhesively bonded secondary barrier of LNG containment system whose adherends were composed of an aluminum sheet and a stainless steel foils, was investigated. A modified lap shear test specimen and DCB test specimen for thin metal foil was devised to measure the bonding strength and fracture toughness accurately at the cryogenic temperature of -150℃. The effects of adhesive thickness on the bond strength were measured from which it was concluded that the bond strength decreased in adhesive thickness increased due to the low fracture toughness and inherent thermal stress in the adhesive layer. The repeated thermal shock test including LNG immersion test revealed that the adhesive thickness of 0.15 mm had higher bond strength at the cryogenic condition than that of a thicker thickness and it showed a longer endurance against repeated thermal shocks. To increase the fracture toughness for thick adhesive, the effects of glass fiber reinforcement were also investigated. The fiber reinforced adhesive had higher lap shear strength compared with unreinforced adhesive. However, the lap shear strengths with different fiber volume fraction were not changed considerably. On the other hand, the fracture toughness with fiber reinforcement increased significantly with respect to fiber volume fraction. In the real application, the control of the adhesive thickness around 0.15 mm might not be practical, then the fiber reinforcement might be another choice from the view point of practical application.

Acknowledgements

This research was supported by WCU(World Class University) program through the National Research Foundation of Korea funded by the Ministry of

Education, Science and Technology (R31-2008-000-10045-0), grant No. EEWS-2011-N01110017 from EEWS Research Project of the office of KAIST EEWS Initiative (EEWS: Energy, Environment, Water, and Sustainability) and BK21.

References

[1] International Code for the Construction and Equipment of Ships Carrying Liquefied Gases in Bulk (IGC code), Chapter 4, IMO Publications, London (1986).

[2] J. G. Kim, S. W. Park, S. H. Yoon and D. G. Lee, J. Adhesion Sci. Technol. 24, 775-787 (2010).

[3] ASTM D1002-05, Standard Test Method for Apparent Shear Strength of Single-Lap-Joint Adhesively Bonded Metal Specimens by Tension Loading (Metal-to-Metal), ASTM International (2005).

[4] D. Zenkert, An Introduction to Sandwich Construction, Chapter 3, EMAS Publishing, London (1997).

[5] ASTM D3433-99, Standard Test Method for Fracture Strength in Cleavage of Adhesives in Bonded Metal Joints, ASTM International (1999).

[6] S. H. Yoon, B. C. Kim, K. H. Lee, D. G. Lee, J adhes Sci and Tech. 24, 429 (2010).

[7] G. Baravian, D. Chaleix, P. Choquet, P.L. Nauche, V. Puech and M. Rozoy, Surface Coatings Technol. 115, 66-69 (1999).

[8] A.J. Kinloch, Adhesion and Adhesives: Science and Technology, Chapman and Hall, New York (1987).

[9] V. Pocius, Adhesion and Adhesives Technology: An Introduction, Hanser Publishers, Cincinnati, Ohio (1997).

[10] Raymond G.Boeman, Donald Erdman, Lynn Klett and Ronny Lomax, Advanced composites conference. Detroit. MI.(1999).

[11] T.L Anderson, Fracture Mechanics, CRC press (2005).

[12] J Roni and J Chauvin, The General Electric - Technigaz Mark III Containment System, GASTECH, Monaco (1978).

[13] D. G. Lee and N. P. Suh, Axiomatic Design and Fabrication of Composite Structures: Applications in Robots, Machine Tools and Automobiles, pp. 374-375, Oxford University Press (2005).

[14] W. D. Bascom and R. L. Cottington, J adhesion. 7, 333 (1976).

[15] R. F. Wegman, Surface Preparation Techniques for Adhesive Bonding, Noyes Publications, New Jersey, U.S.A. (1989).